Supporting Information

Iron(III) azadiphenolate compounds in a new family of spin crossover iron(II)–iron(III) mixed-valent complexes

Wasinee Phonsri [1], David S. Macedo [1], Barnaby A. I. Lewis [1,2], Declan F. Wain [1]and Keith S. Murray [1,*]

[1] School of Chemistry 17 Rainforest Walk, Monash University, Clayton, VIC 3800 Australia; wasinee.phonsri@monash.edu (W.P.), David.Macedo@csiro.au (D.S.M), dfwai1@student.monash.edu (D.F.W)

[2] Department of Chemistry, University of Warwick, Coventry CV4 7AL, UK; B.Lewis@warwick.ac.uk (B.A.I.L)

* Correspondence: Keith.Murray@monash.edu; Tel.: +613-9905-4512 Fax: +613-9905-4597

Table of Contents

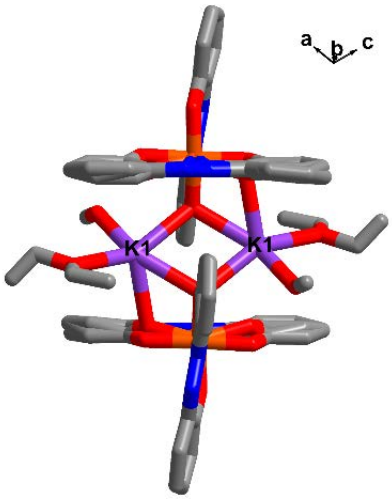

a

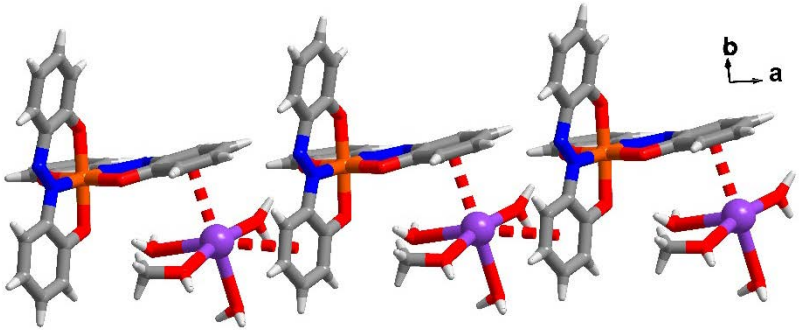

b

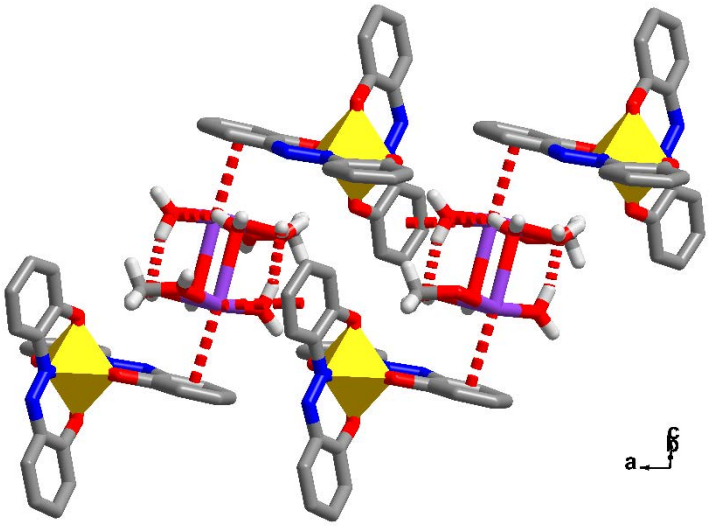

c

Figure S1 a) A dimer of $[Fe(azp)_2]^-$ moieties linking *via* K^+ cations in **1-ref** [1], and b) the K^+ ions forming η_4 interactions to aromatic rings of **1**, and c) {K-OH_2···O(phenolate)-Fe} hydrogen-bonding pathways in **1**.

Table S1 Crystallographic data and structure refinement for **1, 2,** and **3**

	1	**2**	**3**	
	123 K	**123 K**	**100 K**	**300 K**
Formula	$C_{25}H_{26}FeKN_4O_8$	$C_{20}H_{20}Cl_2FeN_{12}O_8$	$C_{52}H_{38}Cl_6Fe_3N_{14}O$	$C_{52}H_{38}Cl_6Fe_3N_{14}O$
Molecular weight / gmol-1	605.45	683.23	1255.21	1255.21
Crystal system	Monoclinic	Monoclinic	Triclinic	Triclinic
Space group	$P2_1/n$	$P2_1/n$	$P\bar{1}$	$P\bar{1}$
a / Å	9.8080 (1)	10.2987 (2)	13.060 (3)	13.230 (3)
b / Å	16.7440 (3)	7.5907 (2)	14.650 (3)	14.730 (3)
c / Å	15.6654 (2)	17.3764 (4)	15.310 (3)	15.370 (3)
α / °	90	90	78.29 (3)	78.12 (3)
β / °	93.098 (1)	103.506 (2)	78.75 (3)	78.98 (3)
γ / °	90	90	70.90 (3)	71.00 (3)
Cell volume / Å^3	2568.89 (6)	1320.82 (5)	2684.0 (11)	2746.3 (11)
Z	4	2	2	2
Absorption coefficient / mm^{-1}	6.663	7.086	1.153	1.126
Reflections collected	26214	13697	56946	59154
Independent reflections, R_{int}	5320, 0.1088	2738, 0.0680	15032, 0.0641	15489, 0.0235
Max. and min. transmission	1.00000 and 0.24243	1.00000 and 0.54615	0.966 and 0.933	0.967 and 0.935
Restraints/parameters	3/338	0/196	0/687	0/687
Final R indices [I>2σ(I)]: R_1, wR_2	0.0610, 0.1734	0.0456, 0.1270	0.0666, 0.1915	0.0503, 0.1483
CCDC number	1905259	1905257	1905260	1905261

Table S2 Selected bond length and octahedral distortion parameters for **1-ref** [1]**, 1, 2,**and **3**

1-ref [1]		**1**	
90 K		**123 K**	
Fe-O1/Å	1.971(5)	Fe1-O1/Å	1.928 (3)
Fe-O2/Å	1.890(4)	Fe1-O2/Å	1.878 (2)
Fe-O3/Å	1.928(8)	Fe1-O3/Å	1.925 (2)
Fe-O4/Å	1.949(8)	Fe1-O4 /Å	1.873 (2)
Fe-N1/Å	2.079(6)	Fe1-N1/Å	1.917 (3)
Fe-N2/Å	2.096(8)	Fe1-N3/Å	1.908 (3)
Σ/° (Fe1)	94	Σ/° (Fe1)	36
Θ/° (Fe1)	235	Θ/° (Fe1)	48

2		**3**		
123 K			**100 K**	**300 K**
Fe1-N1/Å	1.9736 (19)	Fe1-N1/Å	1.966 (2)	1.9711 (18)
Fe1-N1^{i}/Å	1.9736 (19)	Fe1-N2/Å	1.877 (2)	1.8771 (17)
Fe1-N2/Å	1.972 (2)	Fe1-N3/Å	1.956 (2)	1.9618 (18)
Fe1-N2^{i}/Å	1.972 (2)	Fe1-N7/Å	1.968 (2)	1.9683 (18)
Fe1-N3/Å	1.970 (2)	Fe1-N8/Å	1.878 (2)	1.8800 (16)
Fe1-N3^{i}/Å	1.970 (2)	Fe1-N9/Å	1.972 (2)	1.9794 (18)
Σ/° (Fe1)	29	Σ/° (Fe1)	80	81
Θ/° (Fe1)	35	Θ/° (Fe1)	240	252

Symmetry code: (i) −*x*+1, −*y*+1, −*z*+1.

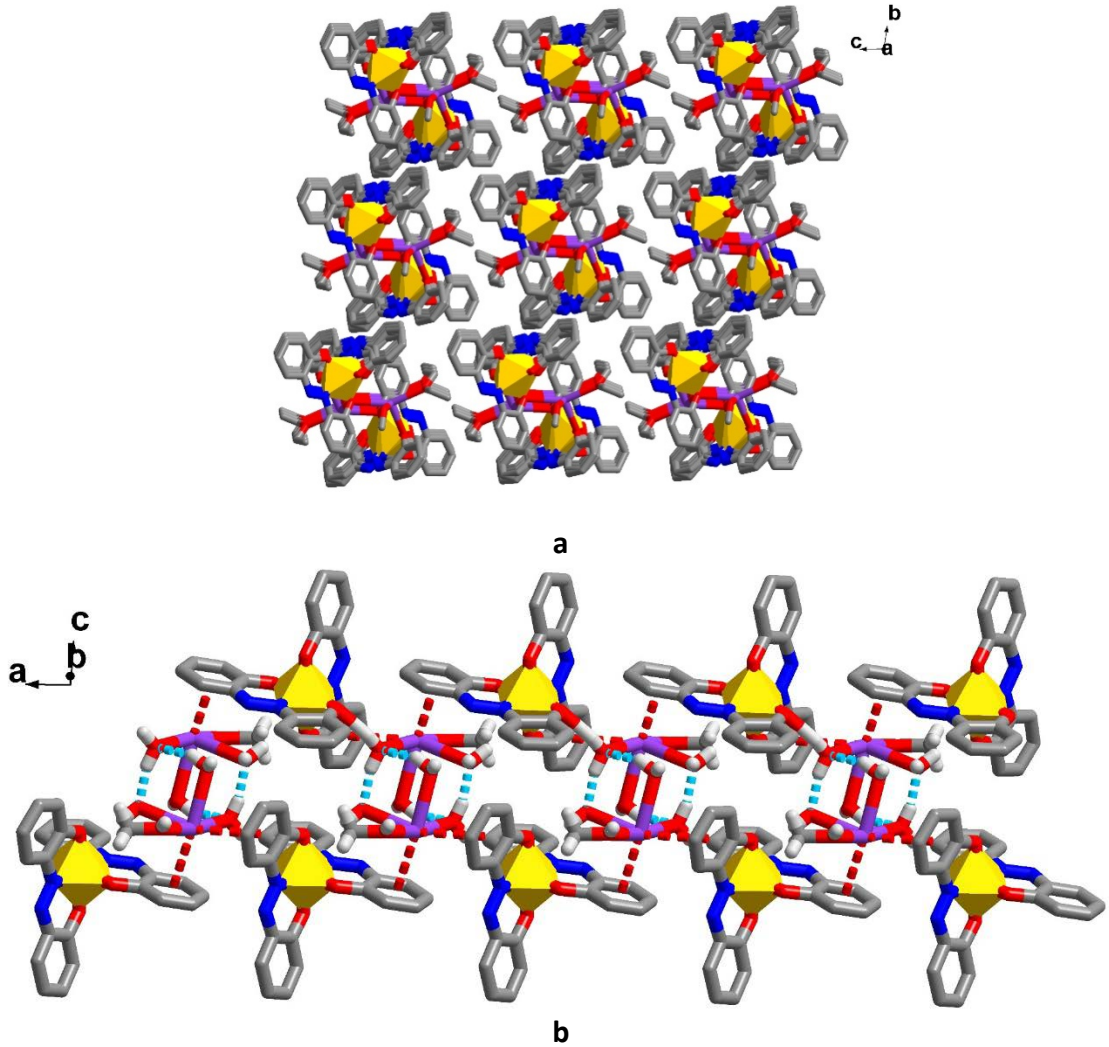

Figure S2 Crystal packing of a) **1-ref**, viewing through the *a*-axis. and b) **1**, viewing through the *b*-axis. Red and blue broken lines represent $K^{+}\cdots\pi$ and O···H interactions, respectively. Hydrogen atoms omitted for clarity

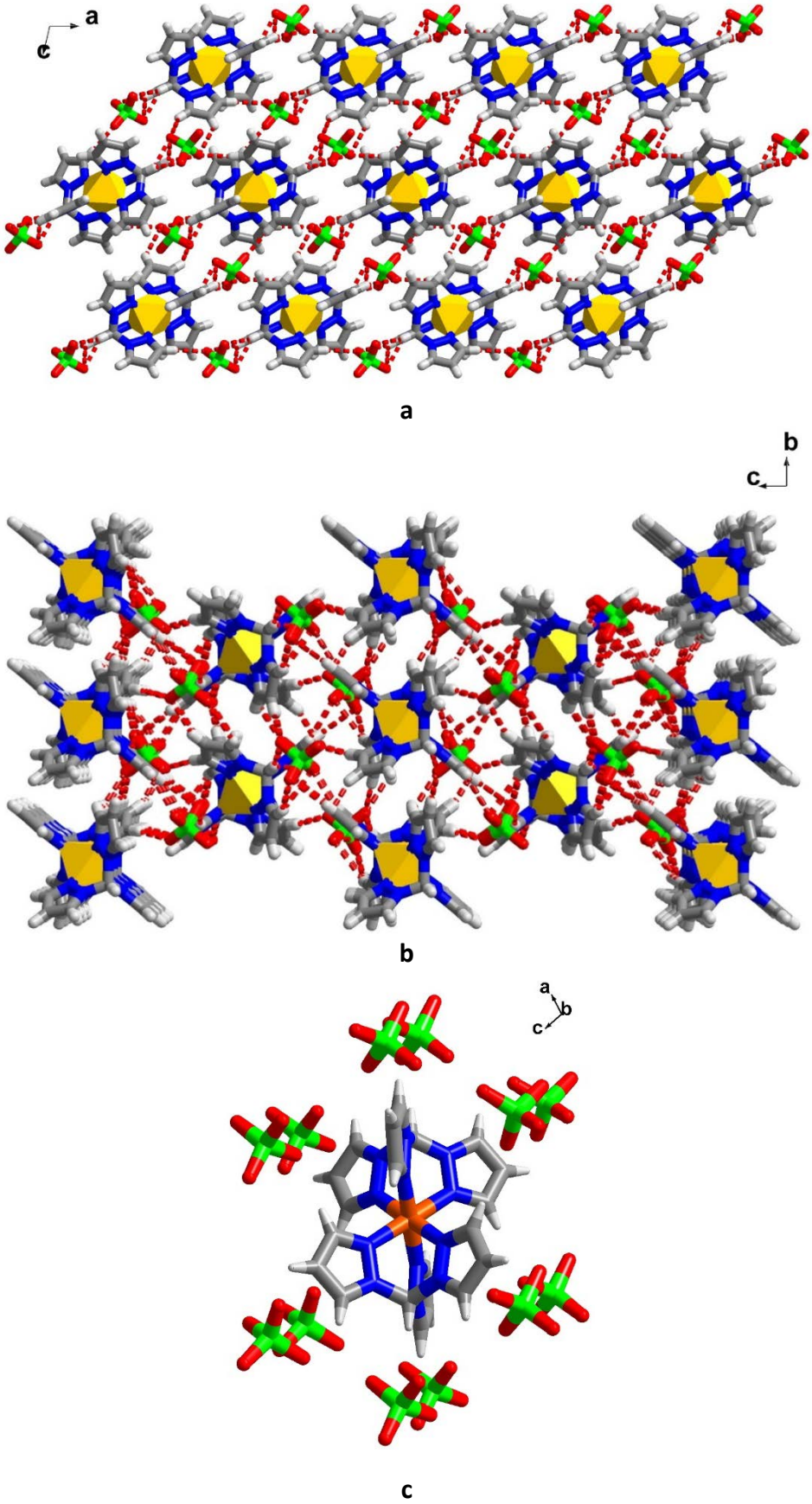

Figure S3 C-H···O interactions between Fe^{II} moieties and ClO_4^- in compound **2** that link Fe^{II} cationic molecules in a) a sheet on *ac* plane and b) a *pseudo*-3D network, c) showing ClO_4^- anions around the $[Fe^{II}\{(pz)_3CH\}_2]^{2+}$ molecule

Table S3 Selected intermolecular interactions in compound **2**. (Å)

Fe^{II} molecules with O from ClO_4 on *ac* sheet	Distance/Å
C3-H3···O1	2.7019(0)
C10-H10···O2	2.2773(0)
C10-H10···O3	2.3585(1)
C4-H4···O1	2.4496(0)
C7-H7···O4	2.3435(0)
Connect the *ac* sheet along the *b* axis	
C2-H2···O2	2.3722(0)
C8-H8···O4	2.4555(0)
C5-H5···O1	2.6629(0)
C6-H6···O3	2.6617(1)

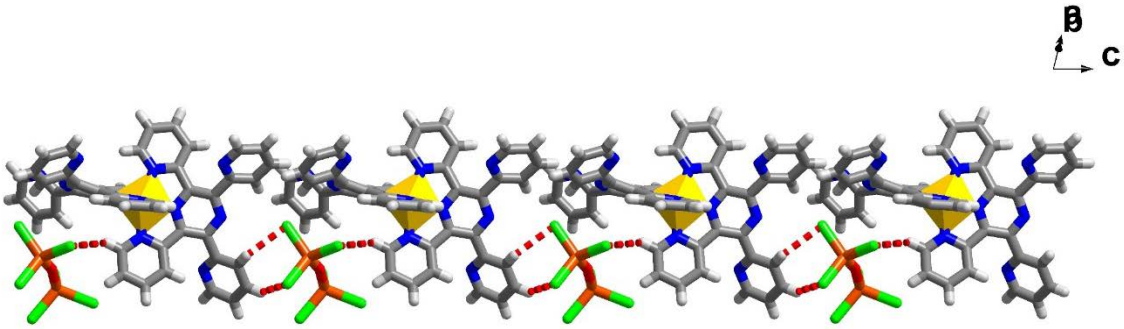

a

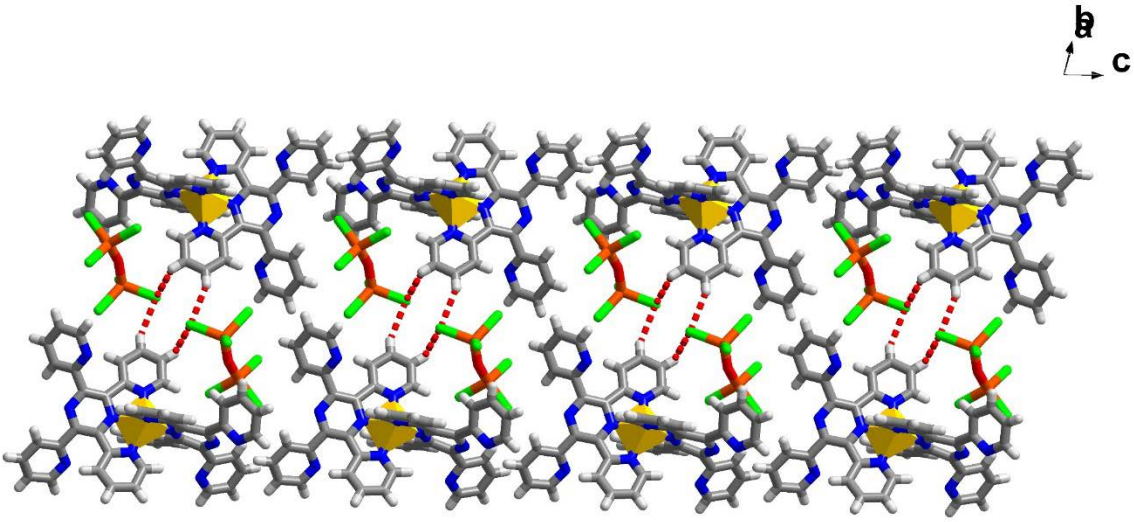

b

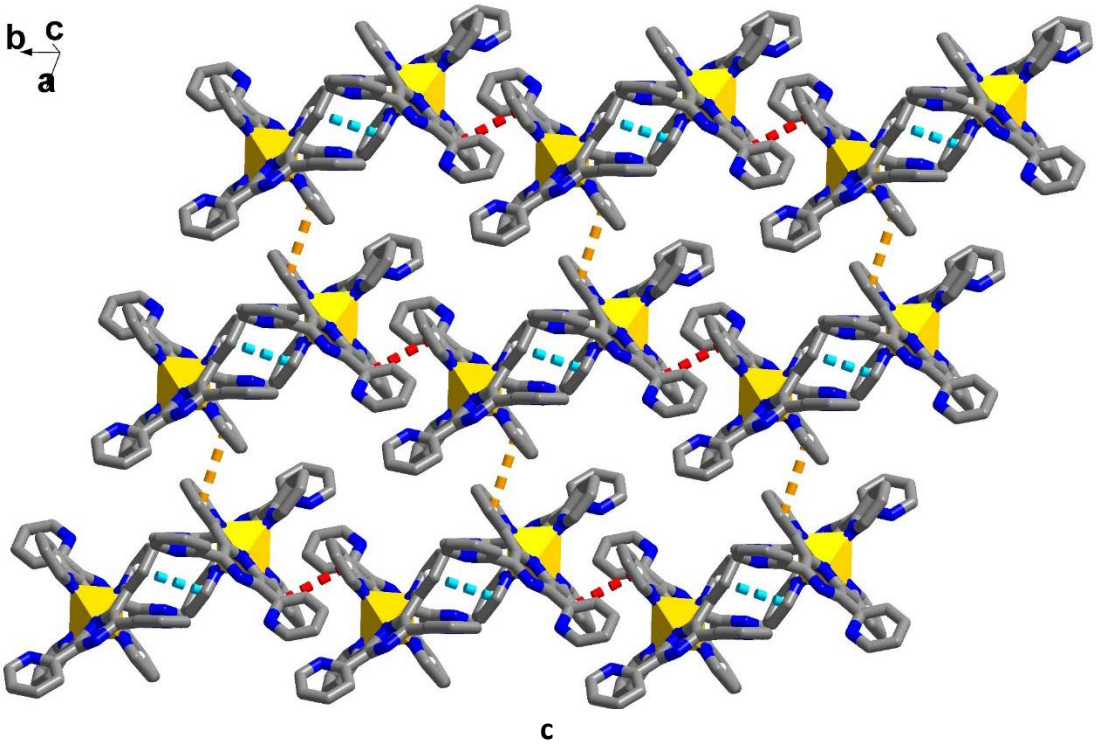

Figure S4 Crystal packing in compound **3** showing the C-H···Cl interactions that connect $[Fe^{II}(TPPZ)_2]^{2+}$in a) a chain along the *c* axis, b) a 2D sheet on an *ac* plane and c) 3 types of P4AE interactions that connect $[Fe^{II}(TPPZ)_2]^{2+}$ along an *ab* plane (P4AE-A: red, P4AE-B: orange and P4AE-C: blue)

Table S4 Selected intermolecular interactions in compound **3**. (Å)

	100 K	**300 K**
Chain along c axis		
C46-H46···N6	2.6725(11)	2.7163(11)
C34-H34···Cl1	2.9321(10)	-
C25-H25···Cl2	2.7432(10)	2.7661(10)
C33-H33···Cl3	2.8920(7)	2.9404(7)
Chain along a axis		
C26-H26···Cl5	2.9461(8)	-
C27-H27···Cl5	2.6863(6)	2.7557(6)
Sheet on ab plane		
P4AE-A		
C15-H15···π	2.514	2.592
π···π	3.377	3.419
P4AE-B		
C3-H3···π	2.618	2.748
π···π	3.281	3.341
P4AE-C		
C39-H39···π	2.554	2.645
π···π	3.443	3.465

Table S5 Selected intermolecular interactions in compound **4**. (Å)

	100 K	**300 K**
A sheet along *ab* plane		
C3-H3···π	2.745	2.881
C22-H22···O1	2.7026(8)	-
π-π	3.407	3.496
C10-H10···π	2.901	-
C14-H14···π	2.701	2.775
A chain along the *c* axis		
C27-H27···N2	2.6158(13)	2.6687(1)
C31-H31···N4	2.6479(9)	2.6970(1)
C32-H32···O1	2.2972(13)	2.3835(1)
π-π	3.916	-
C30-H30···O2	2.3102(10)	2.3439(1)

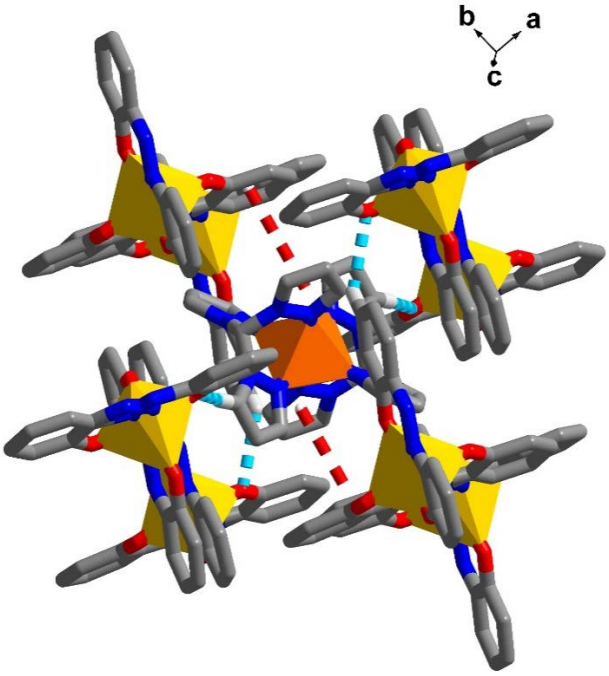

Figure S5 π-π (red broken lines) and C-H···O/N (blue broken lines) interactions connecting the anionic Fe^{II} (orange polyhedra) and Fe^{III} (yellow polyhedra) molecules in compound **4** along the *c* axis.

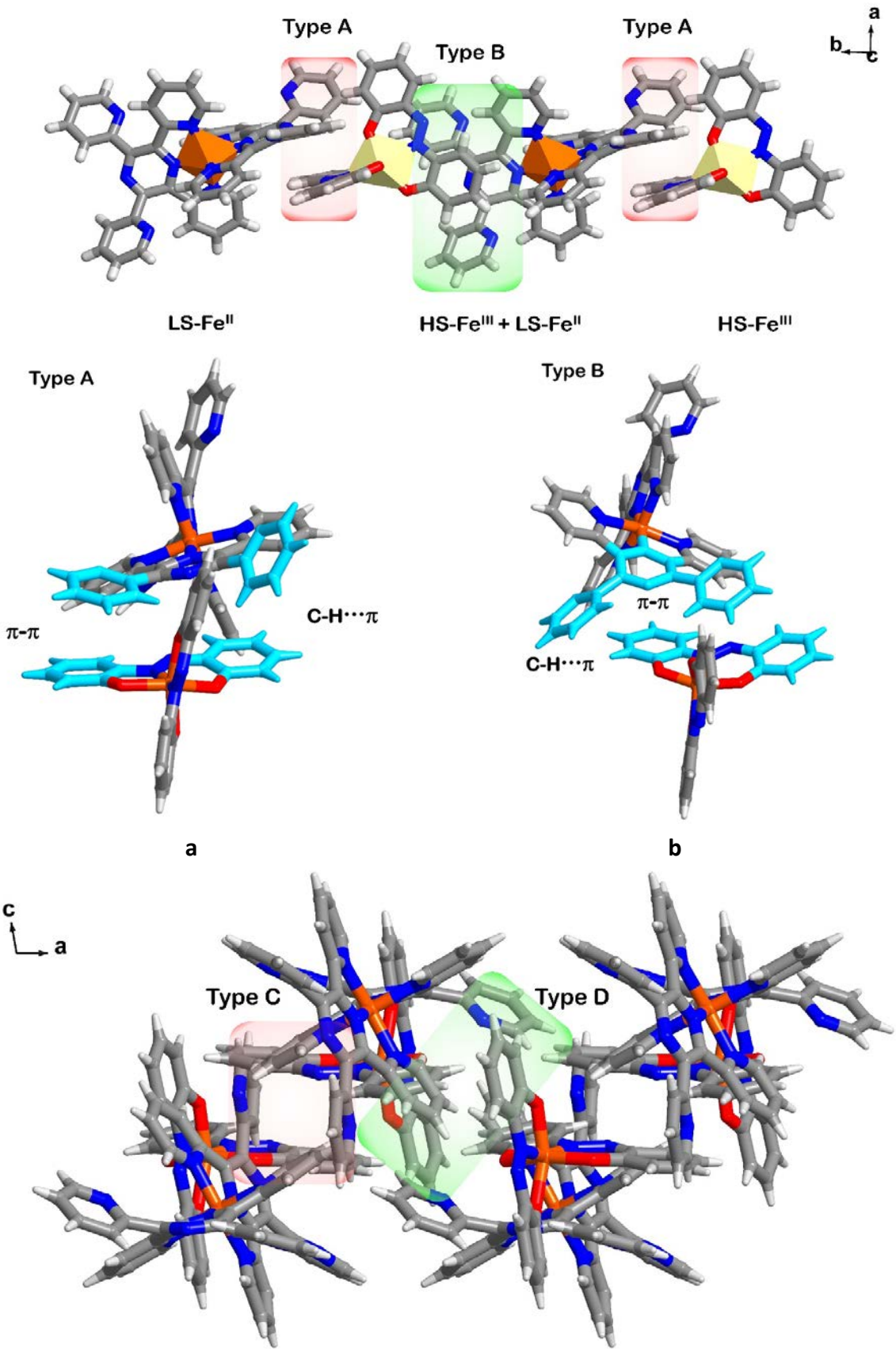
Type A
Type B
Type A
a
b
c
LS-Fe^{II}
HS-Fe^{III} + LS-Fe^{II}
HS-Fe^{III}
Type A
Type B
π-π
C-H···π
π-π
C-H···π
a
b
c
a
Type C
Type D

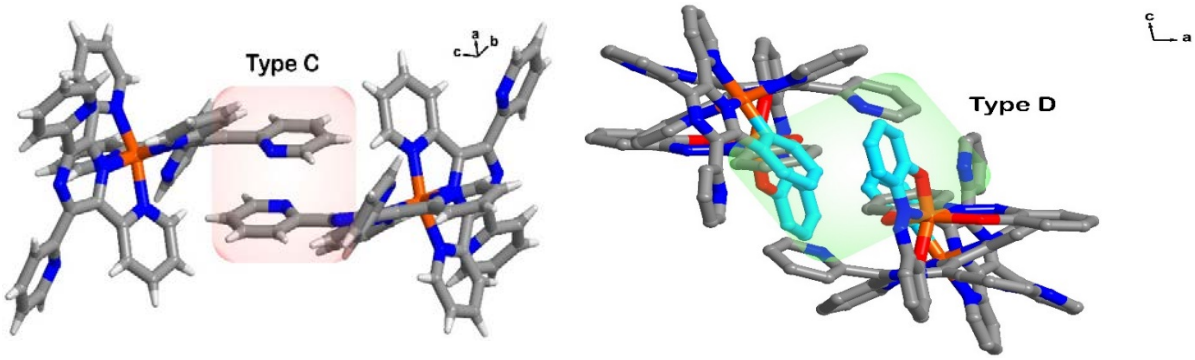

c d

Figure S6 π···π interactions between HS-$[Fe^{III}(azp)_2]^-$; Fe1 and LS-$[Fe^{II}(TPPZ)_2]^{2+}$; Fe3 in compound **5** a) Type A and b) Type B of π···π interactions yielding a 1D chain along the *b* axis. These 1D chains further connect through other two types of π···π interactions *i.e.* c) Type C and d) Type D yielding a 2D layer of HS-$[Fe^{III}(azp)_2]^-$; Fe1 and LS-$[Fe^{II}(TPPZ)_2]^{2+}$; Fe3 on an *ab* plane

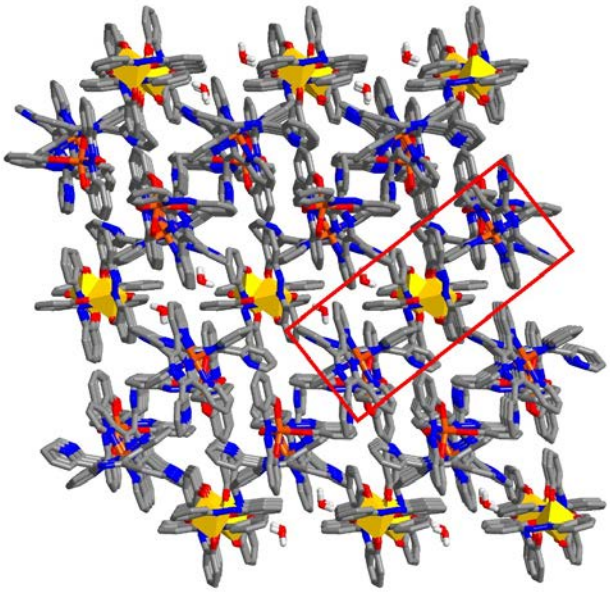

a

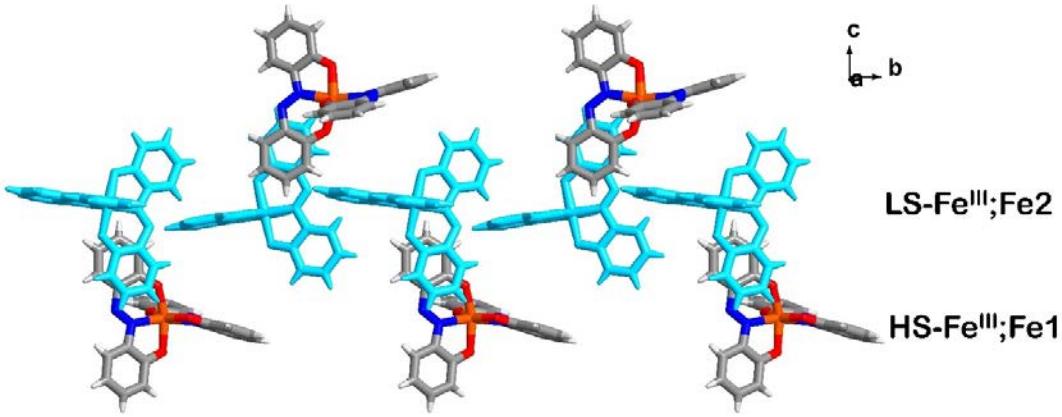

b

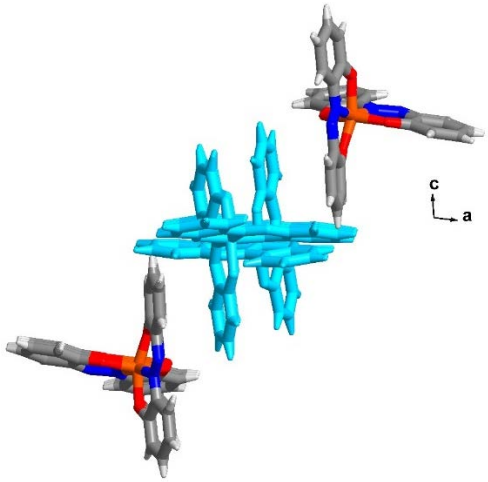

c

Figure S7 a) the crystal packing of **5**, the red rectangle highlights the area of discussion b) π···π interactions between HS-[$Fe^{III}(azp)_2]^-$; Fe1 (blue molecules) and LS-[$Fe^{III}(azp)_2]^-$; Fe2, viewing along the *a* axis and c) a view along the *b* axis of the same chain as b) to clearly show the π···π stackes between two types of [$Fe^{III}(azp)_2]^-$.

Table S6 Selected intermolecular interactions in compound **5**. (Å)

	100 K	**300 K**
Anionic sheet of LS-Fe^{III} on an *ab* plane		
C41-H41···N6	2.6327(4)	2.6663(4)
C46-H46···O9	2.5706(5)	2.6390(6)
O9-H9B···O7	2.0276(4)	1.9941(4)
A chain along the *b* axis, HS-Fe^{III}-LS-Fe^{II}		
Type A		
C84-H84···π	2.762	2.802
π···π	3.598	3.631
Type B		
C2-H2···π	2.806	(2.908)
π···π	3.740	3.784
Between chains of HS-Fe^{III}-LS-Fe^{II}		
Type C		
π···π	3.942	3.926
Type D		
π···π	3.740	3.782
Along the c axis, HS-Fe^{III}-LS-Fe^{III}		
π···π	3.580	3.607

π···π is centroid to centroid distance,
Note for Type C at 100 K, plane to plane distance is 3.62 Å

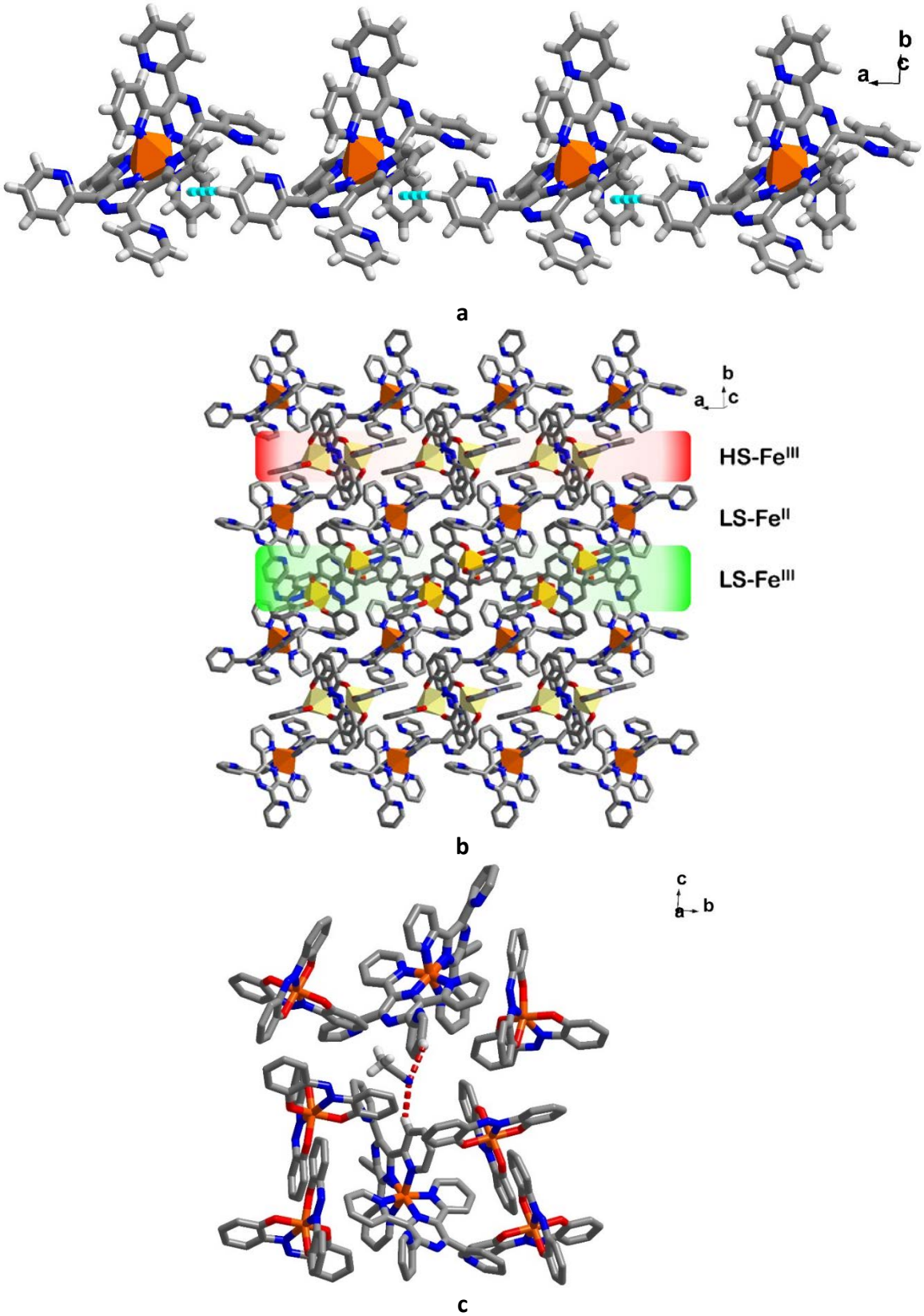

Figure S8 Representation of crystal packing and selected intermolecular interaction in **6**. a) C-H⋯π interactions between LS-Fe^{II} forming a 1D chain along the *a* axis, b) *pseudo*-2D sheet on an *ab* plane, and c) C-H⋯N22 interactions relating to MeCN solvent that link sheets of Fe molecules in forming a *pseudo*-3D network

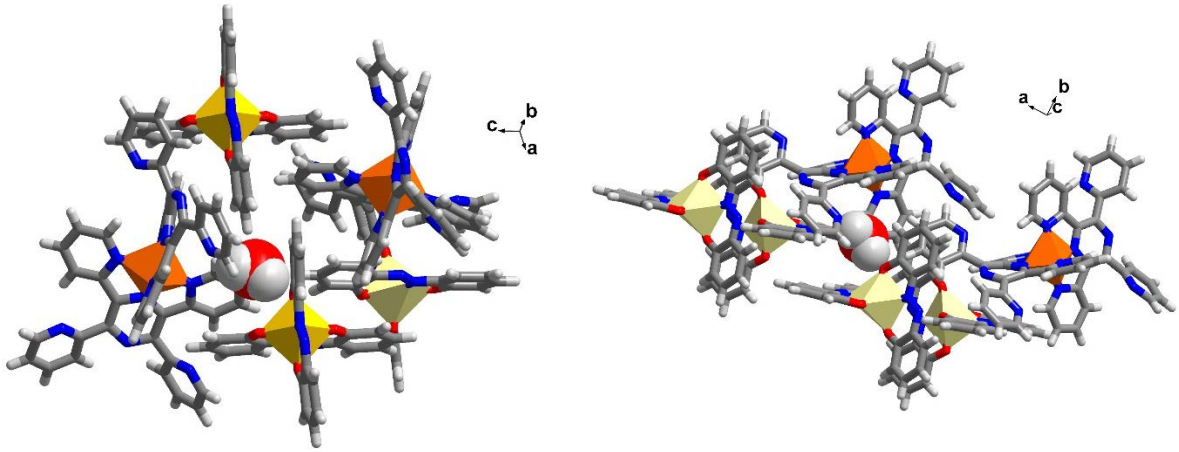

Compound 5 **Compound 6**

Figure S9 Water solvation occupation in the pocket of Fe molecules in **5** and **6**. Light yellow, yellow and orange polyhedra are Fe1(HS-Fe^{III}), Fe2(LS-Fe^{III}) and Fe3(LS-Fe^{II}), respectively.

Table S7 Selected intermolecular interactions in compound **6** (Å)

	100 K	**300 K**
chains along the *a* axis		
C94-H94···π	2.667	2.751
C93-H93···N15	2.5698(5)	2.6131(6)
C74-H74···O6	2.3161(4)	2.3932(4)
C75-H75···π	2.964	(3.060)
C9-H9···π	2.944	3.000
C90-H90···O4	2.5927(4)	2.6633(4)
chains along *b* axis		
C50-H50···π	2.640	2.740
C70-H70···π	2.864	2.949
C65-H65···π	2.638	2.702
Fe2-Fe2		
C38-H38···O8	2.4982(5)	2.6003(4)
C39-H39···N6	2.6899(6)	2.7467(6)
Fe1-Fe1		
C11-H11···O2	2.5522(5)	2.5398(5)
MeCN solvate		
C76-H76···N22	2.6025(7)	2.7375(8)
C58-H58···N22	2.7025(6)	2.7831(7)

Powder diffraction data

All the experiments were performed at room temperature. The PXRD plot for the bulk sample of **5** does not agrees with that simulated from single crystal data, suggesting the bulk sample is not a pure phase. Bulk sample of compound **5** was re-crystallized in MeCN and yielded compound **6.** Experimental PXRD result of **6** is different from that of **5** but agree very well with the simulated PXRD pattern from the single crystal structure of **6**. This suggests the bulk phase of **6** is pure**.**

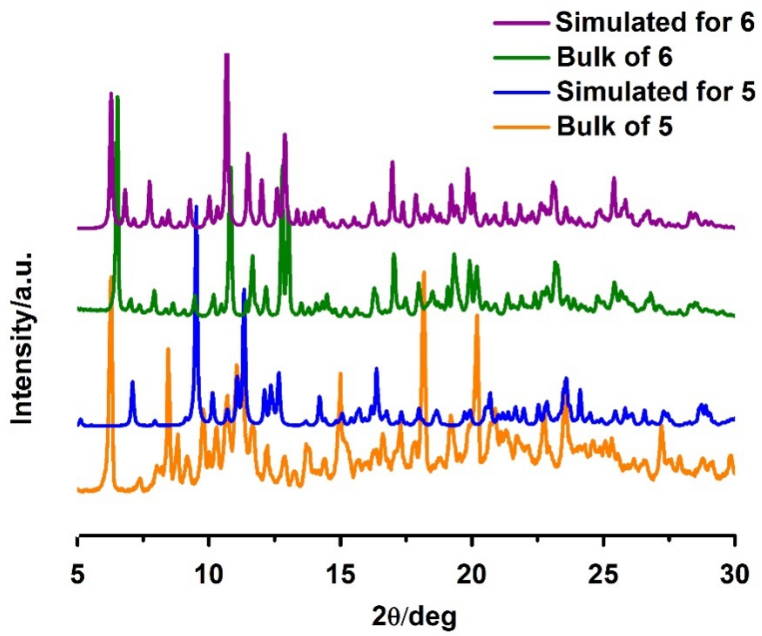

Figure S10 Comparison of PXRD patterns between simulated and experimental PXRD patterns of compound **5** and **6**.

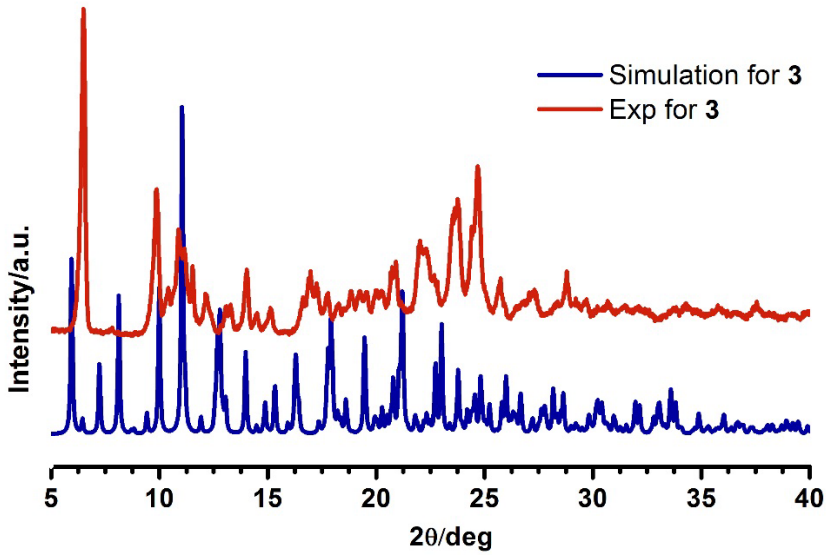

a

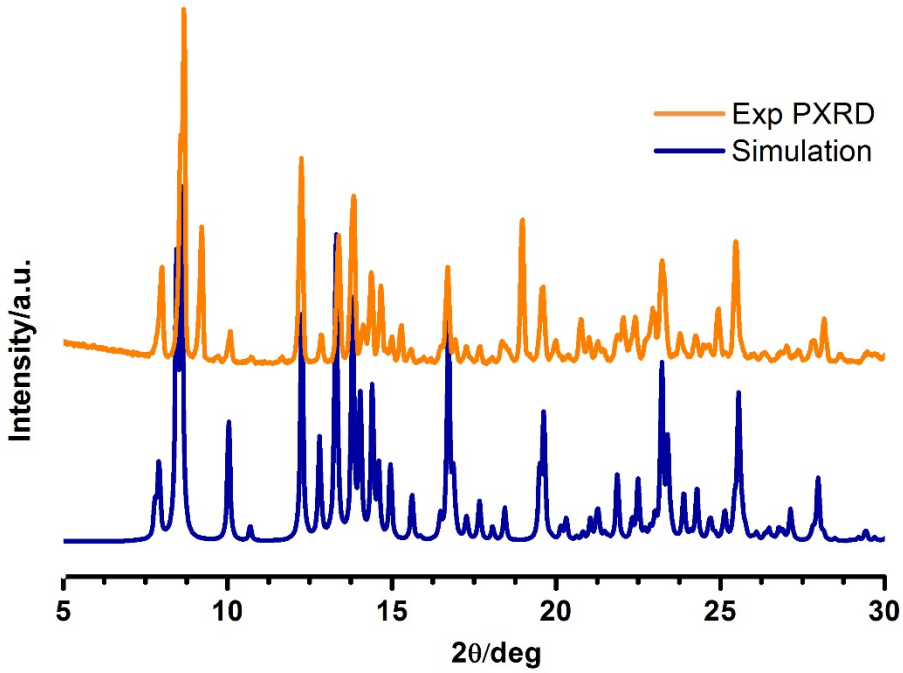

b

Figure S11 Comparison of PXRD patterns between simulated and experimental PXRD patterns of compound a) **3** and b) **4**

References

1. Takahashi, K.; Kawamukai, K.; Okai, M.; Mochida, T.; Sakurai, T.; Ohta, H.; Yamamoto, T.; Einaga, Y.; Shiota, Y.; Yoshizawa, K. A new family of anionic FeIII spin crossover complexes featuring a weak-field N2O4 coordination octahedron. *Chem. Eur. J.* **2016**, *22*, 1253-1257.